The Journal of Chemical Physics

RESEARCH ARTICLE | AUGUST 17 2023

Coupling of orbital and spin polarizations to interatomic hopping in a helical atomic chain

Special Collection: Chiral Induced Spin Selectivity

Yuya Yatabe; Hiroshi Akera

J. Chem. Phys. 159, 074701 (2023)
https://doi.org/10.1063/5.0156461

AIP Publishing

The Journal of Chemical Physics ARTICLE pubs.aip.org/aip/jcp

Coupling of orbital and spin polarizations to interatomic hopping in a helical atomic chain

Cite as: J. Chem. Phys. 159, 074701 (2023); doi: 10.1063/5.0156461
Submitted: 30 April 2023 • Accepted: 1 August 2023 •
Published Online: 17 August 2023

Yuya Yatabe[1] and Hiroshi Akera[2,a)]

AFFILIATIONS

[1] Division of Applied Physics, Graduate School of Engineering, Hokkaido University, Sapporo, Hokkaido 060-8628, Japan
[2] Division of Applied Physics, Faculty of Engineering, Hokkaido University, Sapporo, Hokkaido 060-8628, Japan

Note: This paper is part of the JCP Special Topic on Chiral Induced Spin Selectivity.
[a)]**Author to whom correspondence should be addressed:** akera@eng.hokudai.ac.jp

ABSTRACT

Electron transport through a variety of helical structures has been shown to exhibit high-efficiency spin filtering, which is called chirality-induced spin selectivity (CISS). In this paper, we consider a helical chain of atomic p orbitals, which has been employed as a model in exploring the mechanism of CISS in previous theories, and show that the interatomic hopping along the helical chain induces an effective magnetic field (EMF) acting on the atomic orbital angular momentum (OAM). In chains where the curvature and torsion of the helix are small, we find that the EMF on the binormal component of the atomic OAM is created by the curvature, while that on the tangential component is produced by the torsion. We show that such coupling of the atomic OAM and the interatomic hopping leads to current-induced orbital and spin polarizations. We expect that the present coupling, which is expressed locally, can be used to estimate orbital and spin polarizations locally induced in molecules and solids.

I. INTRODUCTION

A high-efficiency spin filtering has been observed in helical organic molecules such as dsDNA, oligopeptides, and helicene[1–11] and is called chirality-induced spin selectivity (CISS) (see, for a review, Ref. 12). In this paper, we focus on the spin selectivity in electron transport through a single organic molecule,[3,5–7,9–11,13] in which the current at each voltage is larger for the electron spin direction parallel or antiparallel to the current depending on the chirality of the helix. Since the employed organic molecules are nonmagnetic and consist of light elements with small spin–orbit interaction (SOI), the observed high spin selectivity might be caused by an unknown mechanism originating from the helical geometry.

Another important observable quantity, in addition to the flow of spin observed in CISS experiments, is the density of spin due to the current-induced spin polarization. In our previous study,[14] we calculated the spin polarization and the polarization of the atomic orbital angular momentum (OAM) in the presence of current through a chain of atoms along the helix as a model system. This model, a helical atomic chain, which takes into account intra-atomic SOI, has been employed in recent theoretical studies[15,16] on the CISS. We have found there that both polarizations are induced in the direction of the helix axis and are proportional to the curvature when the radius of the helix is much larger than the pitch, that is, the curvature is much larger than the torsion of the helix. This finding suggests that the curvature generates the polarization of the atomic OAM perpendicular to the plane containing the electron trajectory, and this orbital polarization induces spin polarization through the intra-atomic SOI.

There is another parameter, *the torsion*, to define the helical geometry in addition to the curvature. In this paper, we study the dependences on torsion as well as the curvature of polarizations of the atomic OAM and the spin in a helical atomic chain. Here, we calculate the atomic polarizations of the OAM and the spin in the tangential, normal, and binormal directions at the position of each atom on the helix. For this purpose, we describe eigenvectors in a linear combination of atomic p orbitals, $p_{\hat{t}}$, $p_{\hat{n}}$, and $p_{\hat{b}}$, in these directions. First, we derive, from the tight-binding Hamiltonian with nearest-neighbor hopping, the coupling of the interatomic hopping and the atomic OAM in the form of the effective magnetic field (EMF) acting on the atomic OAM. We find that the EMF on the binormal (tangential) OAM is proportional to the curvature κ (torsion τ) in the lowest order of κd and τd with d the interatomic distance. Then we calculate the current-induced polarizations of the

atomic OAM and the spin by taking into account the intra-atomic SOI[14–16] and find that both polarization in the binormal (tangential) direction are proportional to the curvature κ (torsion τ), reflecting the geometry dependence of the EMF on the corresponding OAM.

II. COUPLING OF INTERATOMIC HOPPING AND ATOMIC OAM

We start with a more general system, a chain of atoms on an arbitrary curve. In this section, we focus on the coupling of the interatomic hopping to the intra-atomic OAM without considering the spin degree of freedom. As a basis set for orbitals in each atom, we employ p orbitals, $p_{\hat{t}}$, $p_{\hat{n}}$, and $p_{\hat{b}}$, in the tangential, normal, and binormal directions, respectively, at the position of each atom on the curve. Neighboring $p_{\hat{t}}$ orbitals form σ-like bonding, while neighboring $p_{\hat{n}}$ orbitals and neighboring $p_{\hat{b}}$ orbitals form π-like bondings. The Hamiltonian describing the nearest-neighbor hopping is written as

$$\hat{H}_{\rm hop} = \sum_n \sum_{\alpha,\beta=\hat{t},\hat{n},\hat{b}} \hat{S}|p_\beta n\rangle t_{\beta\, n+1,\alpha n} \langle p_\alpha n| + \text{h.c.}, \tag{1}$$

where n is the number in sequential order of each atom on the curve, the vector $|p_\alpha n\rangle$ $(\alpha = \hat{t}, \hat{n}, \hat{b})$ represents the p_α orbital in the nth atom, and h.c. denotes the Hermitian conjugate of the preceding term. Here, the operator $\hat{S}$, which is defined by

$$\hat{S}|p_\beta n\rangle = |p_\beta n + 1\rangle, \tag{2}$$

increases n by one without changing the orbital β.

Now we restrict our discussion to a chain of atoms that are placed on a helix with equal distances, d, between neighboring atoms (Fig. 1). By choosing the z axis along the helix axis, the coordinates of the nth atom are

$$(x_n, y_n, z_n) = (a\cos n\varphi, a\sin n\varphi, bn\varphi). \tag{3}$$

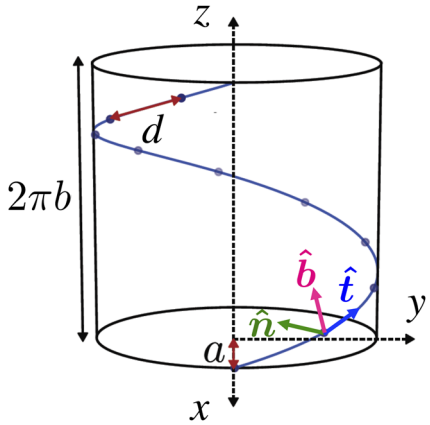

FIG. 1. Chain of atoms on a helix with radius a and pitch $2\pi b$. The curvature and the torsion of the helix are given by $\kappa = a/(a^2 + b^2)$ and $\tau = b/(a^2 + b^2)$, respectively. The interatomic distance d is chosen to be $d = 2.9$ Å for iodine atoms. In addition, shown are tangential $(\hat{t})$, normal $(\hat{n})$, and binormal $(\hat{b})$ directions at an atom.

Here, $a(>0)$ and $2\pi|b|$ are the radius and pitch of the helix, while $\varphi(>0)$ is the increment of the angle around the z axis. The number of atoms per pitch, $2\pi/\varphi$, is not restricted to being an integer. The periodic boundary condition with a periodicity of N is assumed, and the limit of $N \to \infty$ is taken. The sign of b determines the chirality. In the following, we only consider the chirality of $b > 0$.

Owing to the helical symmetry, the Hamiltonian is invariant with respect to the combined operation of the rotation by φ around the z axis and the translation by $b\varphi$ along z. The corresponding operator is $\hat{S}$, defined in Eq. (2). In such helical symmetry, the hopping integral $t_{\beta\ n+1,\alpha n}$ is independent of n, as derived from $t_{\beta\, n+1,\alpha n} = \langle p_\beta n+1|\hat{H}_{\rm hop}|p_\alpha n\rangle = \langle p_\beta n+1|\hat{S}\hat{H}_{\rm hop}\hat{S}^{-1}|p_\alpha n\rangle = \langle p_\beta n|\hat{H}_{\rm hop}|p_\alpha n-1\rangle = t_{\beta n,\alpha\, n-1}$. Then $\hat{H}_{\rm hop}$ reduces to

$$\hat{H}_{\rm hop} = \sum_n \sum_{\alpha,\beta=\hat{t},\hat{n},\hat{b}} \hat{S}|p_\beta n\rangle t_{\beta 1\alpha 0}\langle p_\alpha n| + \text{h.c.} \tag{4}$$

We divide $\hat{H}_{\rm hop}$ into terms of $\alpha = \beta$ and those of $\alpha \neq \beta$,

$$\hat{H}_{\rm hop} = \sum_{\alpha=\hat{t},\hat{n},\hat{b}} \hat{H}_{\alpha\alpha} + \sum_{(\alpha,\beta)=(\hat{t},\hat{n}),(\hat{n},\hat{b}),(\hat{b},\hat{t})} \hat{H}_{\alpha\beta} \tag{5}$$

with

$$\hat{H}_{\alpha\alpha} = \sum_n \hat{S}|p_\alpha n\rangle\, t_{\alpha 1\alpha 0}\, \langle p_\alpha n| + \text{h.c.}, \tag{6}$$

$$\hat{H}_{\alpha\beta} = \sum_n \hat{S}\Big(|p_\beta n\rangle t_{\beta 1\alpha 0}\langle p_\alpha n| + |p_\alpha n\rangle t_{\alpha 1\beta 0}\langle p_\beta n|\Big) + \text{h.c.} \tag{7}$$

In a helical atomic chain, the hopping integral $t_{\beta 1\alpha 0}$ has the following symmetry:

$$t_{\hat{n}1\hat{t}0} = -t_{\hat{t}1\hat{n}0}, \tag{8}$$

$$t_{\hat{b}1\hat{n}0} = -t_{\hat{n}1\hat{b}0}, \tag{9}$$

$$t_{\hat{t}1\hat{b}0} = t_{\hat{b}1\hat{t}0}. \tag{10}$$

First we consider $\hat{H}_{\alpha\beta}$ with $(\alpha,\beta) = (\hat{t},\hat{n})$, which reduces to

$$\begin{aligned}\hat{H}_{\hat{t}\hat{n}} &= t_{\hat{n}1\hat{t}0}\hat{S}\sum_n \Big(|p_{\hat{n}} n\rangle\langle p_{\hat{t}} n| - |p_{\hat{t}} n\rangle\langle p_{\hat{n}} n|\Big) + \text{h.c.} \\ &= t_{\hat{n}1\hat{t}0}(-i)\hat{S}\hat{L}_{\hat{b}} + \text{h.c.}\end{aligned} \tag{11}$$

We find that $\hat{H}_{\hat{t}\hat{n}}$ is the coupling between the interatomic hopping $\hat{S}$ and the binormal component of the atomic OAM. Here, $\hat{L}_\gamma$ $(\gamma = \hat{t},\hat{n},\hat{b})$ is the sum of the OAM of each atom in the γ direction, given by

$$\hat{L}_\gamma = \sum_{n=1}^{N} \hat{L}_{\gamma n} \tag{12}$$

with

$$\hat{L}_{\gamma n} = -i|p_\alpha n\rangle\langle p_\beta n| + \text{h.c.}, \tag{13}$$

where $(\alpha,\beta,\gamma) = (\hat{t},\hat{n},\hat{b}),(\hat{n},\hat{b},\hat{t}),(\hat{b},\hat{t},\hat{n})$.

As a basis vector in the presence of the helical symmetry, we employ an eigenvector of $\hat{S}$ for each of p_α,

$$|p_\alpha \tilde{k}\rangle = \frac{1}{\sqrt{N}} \sum_{n=1}^{N} \exp(i\tilde{k}n)|p_\alpha n\rangle, \tag{14}$$

which satisfies

$$\hat{S}|p_\alpha \tilde{k}\rangle = \exp(-i\tilde{k})|p_\alpha \tilde{k}\rangle. \tag{15}$$

Here, $\tilde{k}$ is the dimensionless momentum. The helical symmetry $[\hat{H}_{\rm hop}, \hat{S}] = 0$ ensures that $\langle p_\beta \tilde{k}'|\hat{H}_{\rm hop}|p_\alpha \tilde{k}\rangle = 0$ when $\tilde{k}' \neq \tilde{k}$, that is $\hat{H}_{\rm hop}$ is diagonal in $\tilde{k}$. Because of the assumed periodic boundary condition with a periodicity of N, the momentum $\tilde{k}$ is quantized into $\tilde{k} = 2\pi j/N$ with j the integer. Since $|p_\alpha \tilde{k} + 2\pi\rangle = |p_\alpha \tilde{k}\rangle$, the value of $\tilde{k}$ is restricted within the first Brillouin zone $|\tilde{k}| < \pi$. With the use of eigenvectors of $\hat{S}$, we can express $\hat{L}_\gamma$ as

$$\hat{L}_\gamma = \sum_{\tilde{k}} \hat{L}_{\gamma\tilde{k}} \tag{16}$$

with

$$\hat{L}_{\gamma\tilde{k}} = -i|p_\alpha \tilde{k}\rangle\langle p_\beta \tilde{k}| + \text{h.c.}, \tag{17}$$

since $\sum_{\tilde{k}} |p_\alpha \tilde{k}\rangle\langle p_\beta \tilde{k}| = \sum_n |p_\alpha n\rangle\langle p_\beta n|$. Then we obtain

$$\begin{aligned}\hat{H}_{\hat{t}\hat{n}} &= t_{\hat{n}1\hat{t}0}(-i)\hat{S}\sum_{\tilde{k}} \hat{L}_{\hat{b}\tilde{k}} + \text{h.c.} \\ &= -\sum_{\tilde{k}} B_{L\hat{b}}(\tilde{k})\, \hat{L}_{\hat{b}\tilde{k}}\end{aligned} \tag{18}$$

with

$$B_{L\hat{b}}(\tilde{k}) = 2t_{\hat{n}1\hat{t}0} \sin\tilde{k}. \tag{19}$$

We find that $\hat{H}_{\hat{t}\hat{n}}$ is the coupling of the binormal OAM $\hat{L}_{\hat{b}\tilde{k}}$ to the momentum $\tilde{k}$ describing transport through the helix, in which $B_{L\hat{b}}(\tilde{k})$ acts on $\hat{L}_{\hat{b}\tilde{k}}$ as an EMF. Similarly, $\hat{H}_{\hat{n}\hat{b}}$ is expressed as

$$\begin{aligned}\hat{H}_{\hat{n}\hat{b}} &= t_{\hat{b}1\hat{n}0}(-i)\hat{S}\hat{L}_{\hat{t}} + \text{h.c.} \\ &= -\sum_{\tilde{k}} B_{L\hat{t}}(\tilde{k})\, \hat{L}_{\hat{t}\tilde{k}}\end{aligned} \tag{20}$$

with

$$B_{L\hat{t}}(\tilde{k}) = 2t_{\hat{b}1\hat{n}0} \sin\tilde{k}. \tag{21}$$

Thus, $\hat{H}_{\hat{n}\hat{b}}$ couples the tangential OAM $\hat{L}_{\hat{t}\tilde{k}}$ to the momentum $\tilde{k}$, and $B_{L\hat{t}}(\tilde{k})$ is the corresponding EMF. On the other hand, $\hat{H}_{\hat{b}\hat{t}}$ produces no terms with the atomic OAM because $t_{\hat{t}1\hat{b}0} = t_{\hat{b}1\hat{t}0}$. Finally, the diagonal-in-orbital component $\hat{H}_{\alpha\alpha}$ is given by

$$\begin{aligned}\hat{H}_{\alpha\alpha} &= t_{\alpha1\alpha0}\hat{S}\sum_{\tilde{k}} |p_\alpha \tilde{k}\rangle\langle p_\alpha \tilde{k}| + \text{h.c.} \\ &= 2t_{\alpha1\alpha0}\sum_{\tilde{k}} \cos\tilde{k}|p_\alpha \tilde{k}\rangle\langle p_\alpha \tilde{k}|,\end{aligned} \tag{22}$$

which shows that $\hat{H}_{\alpha\alpha}$ alone leads to σ-like $p_{\hat{t}}$ bands as well as π-like $p_{\hat{n}}$ and $p_{\hat{b}}$ bands.

The value of the atomic OAM $\hat{L}_{\gamma\tilde{k}}$ ($\gamma = \hat{b}, \hat{t}$) induced by the EMF $B_{L\gamma}(\tilde{k})$ in a state vector $|\psi_{\tilde{k}}\rangle = \sum_{\alpha=\hat{t},\hat{n},\hat{b}} C_{\alpha\tilde{k}}|p_\alpha \tilde{k}\rangle$ is given by

$$\begin{aligned}\langle\psi_{\tilde{k}}|\hat{L}_{\gamma\tilde{k}}|\psi_{\tilde{k}}\rangle &= \langle\psi_{\tilde{k}}|\hat{L}_\gamma|\psi_{\tilde{k}}\rangle = \sum_{n=1}^{N}\langle\psi_{\tilde{k}}|\hat{L}_{\gamma n}|\psi_{\tilde{k}}\rangle \\ &= N\langle\psi_{\tilde{k}}|\hat{L}_{\gamma 0}|\psi_{\tilde{k}}\rangle,\end{aligned} \tag{23}$$

since $\langle\psi_{\tilde{k}}|\hat{L}_{\gamma n}|\psi_{\tilde{k}}\rangle$ does not depend on n as derived from $\langle\psi_{\tilde{k}}|\hat{L}_{\gamma n}|\psi_{\tilde{k}}\rangle = \langle\psi_{\tilde{k}}|\hat{S}\hat{L}_{\gamma n-1}\hat{S}^\dagger|\psi_{\tilde{k}}\rangle = \langle\psi_{\tilde{k}}|e^{-i\tilde{k}}\hat{L}_{\gamma n-1}e^{i\tilde{k}}|\psi_{\tilde{k}}\rangle = \langle\psi_{\tilde{k}}|\hat{L}_{\gamma n-1}|\psi_{\tilde{k}}\rangle$. Therefore, $B_{L\gamma}(\tilde{k})$ induces an equal OAM in each atom. Since the EMF is an odd function of $\tilde{k}$: $B_{L\gamma}(\tilde{k}) = -B_{L\gamma}(-\tilde{k})$, the same is the case for the induced atomic OAM: $\langle\psi_{\tilde{k}}|\hat{L}_\gamma|\psi_{\tilde{k}}\rangle = -\langle\psi_{-\tilde{k}}|\hat{L}_\gamma|\psi_{-\tilde{k}}\rangle$. Thus, the atomic OAM does not appear in equilibrium. However, in the presence of the electric or thermal current through the helix, the difference in electron population between $\tilde{k}$ and $-\tilde{k}$ leads to a net atomic OAM. In Sec. III, we present the calculated results of orbital and spin polarizations induced by the electric current.

We express hopping integrals with the use of the Slater–Koster parameters[17] $V_{pp\pi}(<0)$ and $V_{pp\sigma}(>0)$. Applying the formula in Ref. 18, the hopping integral $t_{\beta1\alpha0}$ is given by

$$t_{\beta1\alpha0} = \boldsymbol{e}_{\beta1}\cdot\boldsymbol{e}_{\alpha0}V_{pp\pi} + (\boldsymbol{e}_{10}\cdot\boldsymbol{e}_{\beta1})(\boldsymbol{e}_{10}\cdot\boldsymbol{e}_{\alpha0})(V_{pp\sigma} - V_{pp\pi}), \tag{24}$$

where $\boldsymbol{e}_{\alpha n}$ is the unit vector in the $\alpha\,(=\hat{t},\hat{n},\hat{b})$ direction at the nth atom and $\boldsymbol{e}_{10}$ is the unit vector in the direction from the $n = 0$ atom to the $n = 1$ atom given by $\boldsymbol{e}_{10} = (x_1 - x_0, y_1 - y_0, z_1 - z_0)/d$. Using Eq. (24) we calculate the dependence of $t_{\beta1\alpha0}$ on the geometry of the helix described by the radius a and the pitch $2\pi b$ as well as on the interatomic distance d. In expressing the geometry dependence of $t_{\beta1\alpha0}$, we use the curvature κ and the torsion τ given by

$$\kappa = \frac{a}{a^2 + b^2}, \quad \tau = \frac{b}{a^2 + b^2} \tag{25}$$

instead of a and b. To obtain a simple expression for the geometry dependence of $t_{\beta1\alpha0}$, we consider the case of $\varphi \ll 1$, in which $\varphi \approx \sqrt{(\kappa d)^2 + (\tau d)^2}$ and, therefore, $\kappa d \ll 1$ and $\tau d \ll 1$. Then, in the lowest order of κd and τd, we obtain, for $t_{\hat{n}1\hat{t}0}$ in $B_{L\hat{b}}(\tilde{k})$ [Eq. (19)] and $t_{\hat{b}1\hat{n}0}$ in $B_{L\hat{t}}(\tilde{k})$ [Eq. (21)],

$$t_{\hat{n}1\hat{t}0} = -\kappa d\,\frac{V_{pp\pi} + V_{pp\sigma}}{2}, \tag{26}$$

$$t_{\hat{b}1\hat{n}0} = -\tau d\, V_{pp\pi}. \tag{27}$$

Therefore, in the case of $\kappa d \ll 1$ and $\tau d \ll 1$, the binormal OAM is proportional to $\kappa d \sin\tilde{k}$, while the tangential OAM is proportional to $\tau d \sin\tilde{k}$. On the other hand,

$$t_{\hat{t}1\hat{b}0} = \kappa\tau d^2\left(\frac{V_{pp\pi}}{3} + \frac{V_{pp\sigma}}{6}\right). \tag{28}$$

This shows that the mixing between binormal and tangential p orbitals, $\hat{H}_{\hat{b}\hat{t}}$, is of the second order of φ in the $\varphi \ll 1$ region and is much smaller than $\hat{H}_{\hat{t}\hat{n}}$ and $\hat{H}_{\hat{n}\hat{b}}$, which are of the first order of φ.

III. ORBITAL AND SPIN POLARIZATIONS INDUCED BY CURRENT

We employ the Hamiltonian,

$$\hat{H} = \hat{H}_{\rm hop} + \hat{H}_{\rm so} \tag{29}$$

in calculating orbital and spin polarizations induced by the current. Here, we take into account, in addition to the interatomic hopping $\hat{H}_{\rm hop}$ in Eq. (4), the intra-atomic SOI $\hat{H}_{\rm so}$ given by

$$\hat{H}_{\rm so} = \sum_n \lambda_{\rm so} \hat{\boldsymbol{L}}_n \cdot \hat{\boldsymbol{\sigma}}/2 \tag{30}$$

with $\hat{\boldsymbol{\sigma}} = (\hat{\sigma}_x, \hat{\sigma}_y, \hat{\sigma}_z)$ the Pauli spin operator. We use atomic parameters for iodine. In determining $\lambda_{\rm so}$ the strength of the intra-atomic SOI, we employ the value of the spin–orbit splitting in p levels, $3\lambda_{\rm so}/2 = 1.029$ eV, in Ref. 19. In the interatomic hopping $\hat{H}_{\rm hop}$, we use values of the Slater–Koster parameters, $V_{{\rm pp}\sigma} = 2.282$ eV and $V_{{\rm pp}\pi} = -0.549$ eV, which have been obtained in Ref. 20, so as to reproduce energy bands of a straight linear iodine chain with $d = 2.9$ Å in the density functional calculation.

Since we include the SOI $\hat{H}_{\rm so}$ in the Hamiltonian, we choose basis vectors that satisfy

$$\hat{S}|{\rm p}_\alpha \sigma \tilde{k}\rangle = \exp(-i\tilde{k})|{\rm p}_\alpha \sigma \tilde{k}\rangle \tag{31}$$

by taking into account the spin degree of freedom. Then the basis vector $|{\rm p}_\alpha \sigma \tilde{k}\rangle$ is expressed by[21]

$$|{\rm p}_\alpha \sigma \tilde{k}\rangle = \frac{1}{\sqrt{N}} \sum_{n=1}^{N} \exp(i\tilde{k}n) \hat{S}^n |{\rm p}_\alpha \sigma 0\rangle \tag{32}$$

with $|{\rm p}_\alpha \sigma 0\rangle = |{\rm p}_\alpha 0\rangle|\sigma\rangle$ and $\hat{S}^n|{\rm p}_\alpha 0\rangle = |{\rm p}_\alpha n\rangle$. Here, $|\sigma\rangle$ is the eigenvector of $\hat{\sigma}_z$, the z component of the Pauli spin operator, satisfying $\hat{\sigma}_z|\sigma\rangle = \sigma|\sigma\rangle$ with eigenvalue $\sigma = \pm 1$. The operation $\hat{S}$ on $|\sigma\rangle$ is given by

$$\hat{S}|\sigma\rangle = \exp(-i\varphi\sigma/2)|\sigma\rangle, \tag{33}$$

since $\hat{S}$ is the rotation by φ around the z axis and the translation by $b\varphi$ along z. Eigenvalues and eigenvectors of $\hat{H}$ are obtained by diagonalizing the 6×6 matrix with elements $\langle {\rm p}_{\alpha'} \sigma' \tilde{k}|\hat{H}|{\rm p}_\alpha \sigma \tilde{k}\rangle$ ($\alpha, \alpha' = \hat{t}, \hat{n}, \hat{b}$ and $\sigma, \sigma' = \pm 1$). Calculated eigenvalues as a function of $\tilde{k}$ of the helical atomic chain with $\kappa = 0.1$ Å^{-1} and $\tau = 0.01$ Å^{-1} are presented in Fig. 2.

Now we calculate orbital and spin polarizations in the presence of an electric current, which is generated at absolute zero by the chemical potential difference: the chemical potential of channels with a velocity in the positive z direction is higher by $\Delta\mu$ than that in the negative z direction. Such electron distribution is obtained in the ballistic transport induced by the chemical-potential difference $\Delta\mu$ between the source and drain electrodes in the Landauer formalism. Induced orbital and spin polarizations of each atom divided by $\Delta\mu$ are given, in the linear response (that is, in the limit of $\Delta\mu \to 0$), by

$$P_{L\gamma} = \sum_{v\tilde{k}}^{v>0} \langle v\tilde{k}|\hat{L}_{\gamma 0}|v\tilde{k}\rangle \delta(E_{v\tilde{k}} - E_F), \tag{34}$$

$$P_{S\gamma} = \sum_{v\tilde{k}}^{v>0} \langle v\tilde{k}|\frac{1}{2}\hat{\sigma}_{\gamma 0}|v\tilde{k}\rangle \delta(E_{v\tilde{k}} - E_F), \tag{35}$$

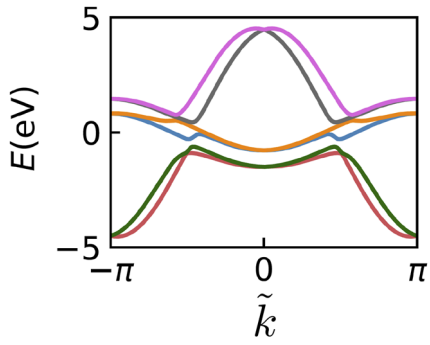

FIG. 2. Energy bands of the helical atomic chain with $\kappa = 0.1$ Å^{-1} and $\tau = 0.01$ Å^{-1}.

for the $\gamma\,(= \hat{t}, \hat{n}, \hat{b})$ component, where $E_{v\tilde{k}}$ and $|v\tilde{k}\rangle$ are the energy and the vector, respectively, of the eigenstate with band index v at momentum $\tilde{k}$, E_F is the Fermi energy, and $\hat{\sigma}_{\gamma 0} = \hat{\boldsymbol{\sigma}} \cdot \boldsymbol{e}_{\gamma 0}$ with $\hat{\boldsymbol{\sigma}}$ the Pauli spin operator.

Figure 3 shows the Fermi energy E_F dependence of binormal orbital polarization $P_{L\hat{b}}$ and tangential orbital polarization $P_{L\hat{t}}$

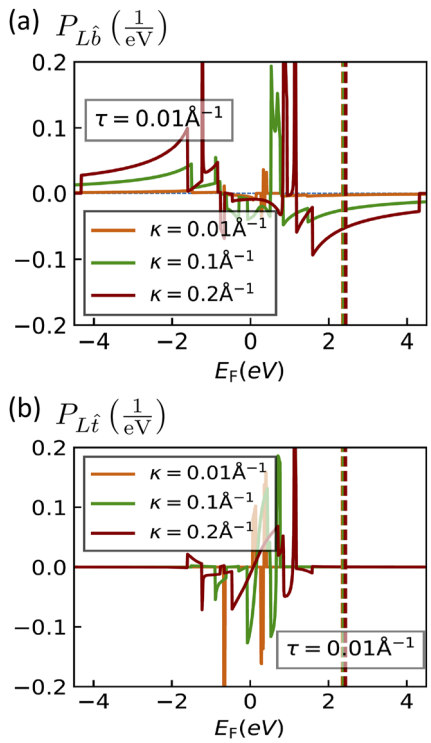

FIG. 3. Orbital polarization induced by current as a function of the Fermi energy E_F: (a) binormal component $P_{L\hat{b}}$ and (b) tangential component $P_{L\hat{t}}$. Vertical dashed lines indicate the Fermi energy corresponding to the fixed electron density, which is used in calculating dependences on κ and τ in Figs. 4–6.

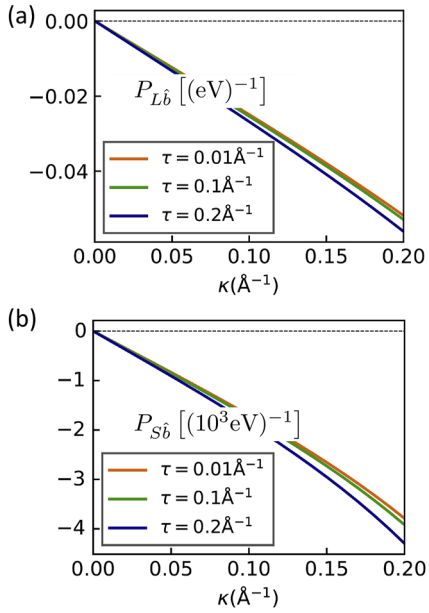

FIG. 4. Binormal component of (a) orbital polarization $P_{L\hat{b}}$ and (b) spin polarization $P_{S\hat{b}}$ induced by current as a function of κ.

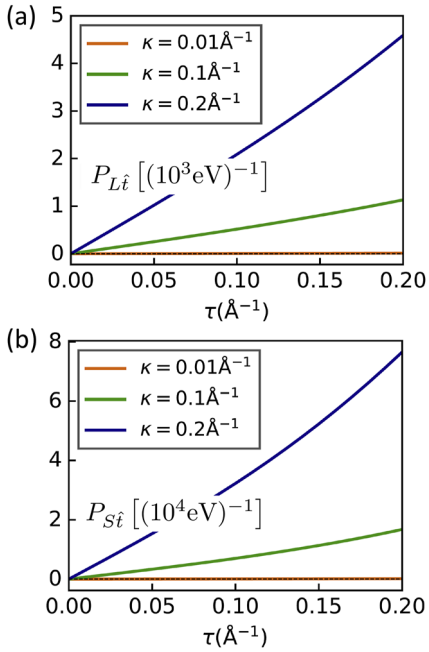

FIG. 5. Tangential component of (a) orbital polarization $P_{L\hat{t}}$ and (b) spin polarization $P_{S\hat{t}}$ induced by current as a function of τ.

induced by current. Orbital polarizations (and similarly spin polarizations) depend strongly on Fermi energy, reflecting the orbital character of each energy band. In the following, we focus on the σ-like band, which is mainly formed by $p_{\hat{t}}$ orbitals. The location of the corresponding Fermi energy is indicated by the vertical dashed line in Fig. 3.

Figure 4 presents the curvature κ dependence of binormal polarizations $P_{L\hat{b}}$ and $P_{S\hat{b}}$ at values of torsion $\tau(\text{Å}^{-1}) = 0.01$, 0.1, and 0.2. We find that binormal polarizations are proportional to κ in the small κ region with weak τ dependences. The linear-in-κ dependence of $P_{L\hat{b}}$ is consistent with the linear-in-κ dependence of the strength $t_{\hat{n}1\hat{t}0}$ [Eq. (26)] of the EMF $B_{L\hat{b}}(\tilde{k})$ in Eq. (19). Since the orbital polarization acts as an EMF on the spin, the linear-in-κ dependence of $P_{L\hat{b}}$ leads to that of $P_{S\hat{b}}$.

Figures 5 and 6 present the τ and κ dependences, respectively, of tangential polarizations $P_{L\hat{t}}$ and $P_{S\hat{t}}$. We find that tangential polarizations are proportional to $\tau\kappa^2$ in the region of $\tau d \ll 1$ and $\kappa d \ll 1$. This dependence can be understood as follows: Energy bands that cross E_F are of the σ-band character and are formed, in the limit of straight linear atomic chains ($\kappa \to 0$ and $\tau \to 0$), by $p_{\hat{t}}$ orbitals, which have a zero eigenvalue of the tangential OAM. In the presence of κd ($\ll$1) and τd ($\ll$1), the tangential-normal mixing $\hat{H}_{\hat{t}\hat{n}}$ with strength $t_{\hat{n}1\hat{t}0} \propto \kappa$ [Eq. (26)] induces $p_{\hat{n}}$ component and the binormal-tangential mixing $\hat{H}_{\hat{b}\hat{t}}$ with strength $t_{\hat{t}1\hat{b}0} \propto \kappa\tau$ [Eq. (28)] induces $p_{\hat{b}}$ component. The tangential polarization of OAM $P_{L\hat{t}}$ formed by $p_{\hat{n}}$ and $p_{\hat{b}}$ components is, therefore, proportional to $\tau\kappa^2$.

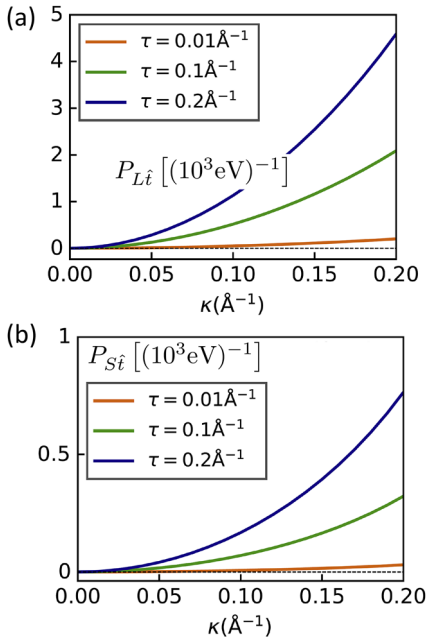

FIG. 6. Tangential component of (a) orbital polarization $P_{L\hat{t}}$ and (b) spin polarization $P_{S\hat{t}}$ induced by current as a function of κ.

IV. DISCUSSION

A. Extending to slowly-varying curvature and torsion

We go back to the hopping Hamiltonian of a chain of atoms on a general curve given in Eq. (1). When variations along the curve of the curvature and the torsion are slow enough that

$$\frac{d\kappa(s)}{ds}d \ll \kappa(s), \quad \frac{d\tau(s)}{ds}d \ll \tau(s), \tag{36}$$

(s is the coordinate along the curve), the hopping integral $t_{\beta n+1,\alpha n}$ approximately satisfies $t_{\hat{n}\,n+1,\hat{t}n} = -t_{\hat{t}\,n+1,\hat{n}n}$ and $t_{\hat{b}\,n+1,\hat{n}n} = -t_{\hat{n}\,n+1,\hat{b}n}$. Then, even in the absence of the helical symmetry, $\hat{H}_{\hat{t}\hat{n}}$ reduces to

$$\begin{aligned}\hat{H}_{\hat{t}\hat{n}} &\approx \sum_n t_{\hat{n}\,n+1,\hat{t}n}\hat{S}\left(|\mathrm{p}_{\hat{n}}n\rangle\langle \mathrm{p}_{\hat{t}}n| - |\mathrm{p}_{\hat{t}}n\rangle\langle \mathrm{p}_{\hat{n}}n|\right) + \text{h.c.} \\ &= \sum_n t_{\hat{n}\,n+1,\hat{t}n}(-i)\hat{S}\hat{L}_{\hat{b}n} + \text{h.c.}\end{aligned} \tag{37}$$

Thus, the binormal OAM in the nth atom, $\hat{L}_{\hat{b}n}$, locally couples to the interatomic hopping with strength $t_{\hat{n}\,n+1,\hat{t}n}$ proportional to the local curvature. Similarly, the tangential OAM, $\hat{L}_{\hat{t}n}$, couples to the interatomic hopping with strength $t_{\hat{b}\,n+1,\hat{n}n}$ proportional to the local torsion.

B. Extending to non-polar molecules and solids

We expect that the direction and geometry dependence of the EMF obtained in this paper for the helical chain (and approximately helical chain) of atomic p orbitals will be useful in estimating the EMF in many non-polar molecules and solids. In molecules and solids in general, transport paths cross and overlap each other. However, if a particular path dominantly contributes to the current-induced EMF, as illustrated in Fig. 7(a), the EMF can be estimated from the curvature and the torsion of the dominant path. Such a dominant path often winds rapidly. Nevertheless, the local curvature can be defined for a chain of three neighboring atoms, to which the local coupling of $\hat{L}_{\hat{b}n}$ and transport, as expressed in Eq. (37), may be considered.

The EMF at an atom may also be estimated by the sum of contributions from different paths through the atom. In an atomic layer with all atoms in the same plane as shown in Fig. 7(b), for example, any path through an atom has a curvature but no torsion. Then we find, by applying the local coupling Eq. (37) to each path, that the EMF due to the three paths is perpendicular to the plane.

In previous studies,[22–25] the coupling of the atomic OAM and the crystal momentum has been introduced in a system with lattice translational symmetry. Here, we have derived the local coupling Eq. (37) of the atomic OAM and the interatomic hopping with strength expressed by the local curvature and the local torsion. We expect that the present coupling can be used to estimate the spin polarization locally induced by current in a system without lattice translational symmetry.

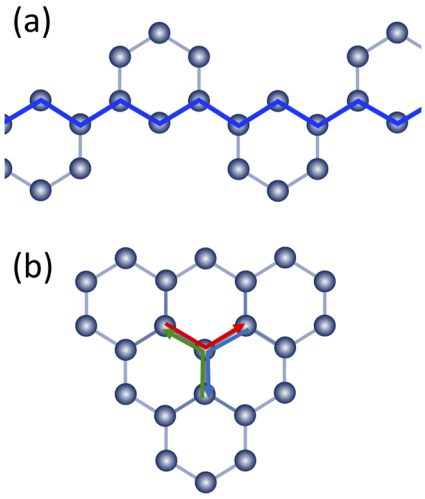

FIG. 7. Transport paths in a molecule and a solid. (a) A molecule with a dominant current path (thick line). (b) Three transport paths (thick lines) through an atom in an atomic layer with all atoms in the same plane.

C. Spin current

Finally, we discuss the spin current induced by connecting another atomic chain to the helical atomic chain, as shown in Fig. 8. The connected chain consists of s-orbital atoms with no SOI and is connected at the other end to the drain electrode. By raising the chemical potential of the source electrode placed below the helical chain relative to that of the drain electrode, electrons flow upward along the helical chain, and spin polarization is induced in each atom of the helical chain. By connecting the s-orbital chain to the helical chain, some electrons diffuse into the connected chain, carrying the spin polarization in the atom at the connecting point. Then, electrons, which continue to travel through the helical chain after passing the connecting point, carry the spin polarization in the opposite direction. In this way, the current-induced spin polarization in the helical atomic chain produces the spin current through the connected chain and that through the helical chain, which has the opposite spin polarization and the same order of magnitude.

The calculated magnitude of the spin current exhibits its maximum as a function of the hopping integral between the helical chain and the connected chain. We find, in the calculation at absolute zero for the helical iodine chain, that the magnitude of the spin current J_s, expressed by a conductance, $G_s = (2e/\hbar)J_s/V_{\mathrm{SD}}$, with V_{SD} the source–drain voltage, reaches $G_s = 0.1G_0$ with $G_0 = e^2/h$ by adjusting the interchain hopping integral. Since $G_s = G_0$ in the 100% spin selectivity, $G_s = 0.1G_0$ means 10% spin

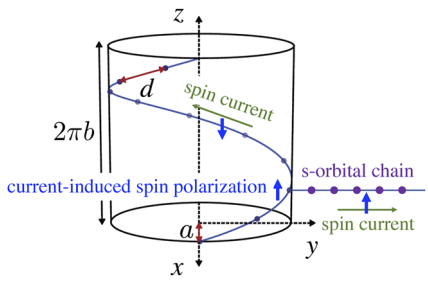

FIG. 8. Spin current induced by connecting an s-orbital chain to the helical chain.

selectivity, which is much smaller than the spin selectivity of greater than 50% observed in CISS experiments. To explain such a large magnitude of the spin selectivity observed in organic molecules with small SOI at room temperature, we need further theoretical studies with consideration of other effects, which may include electron–phonon and electron–electron interactions.

V. CONCLUSIONS

We have considered a helical chain of atomic p orbitals and derived, from the hopping term of the tight-binding Hamiltonian, the coupling between the atomic OAM operator $\hat{\boldsymbol{L}}_n$ of the nth atom and the hopping operator $\hat{S} = \sum_n \sum_{\alpha=\hat{t},\hat{n},\hat{b}} |\mathrm{p}_\alpha n+1\rangle\langle \mathrm{p}_\alpha n|$, which transfers an electron from an orbital in atom n to the same orbital in atom $n+1$. Since this term couples two local operators with the inversion asymmetry expressed by the curvature and the torsion at the position of each atom, it is also applicable to a chain with slowly-varying curvature and torsion.

In the presence of the helical symmetry in which the associated momentum $\tilde{k}$ is conserved, the present coupling reduces to the coupling of $\tilde{k}$ and $\hat{\boldsymbol{L}}_{\tilde{k}}$, which is expressed by the $\tilde{k}$-dependent EMF acting on $\hat{\boldsymbol{L}}_{\tilde{k}}$. This EMF, which appears due to the inversion asymmetry at each atom, is proportional to the curvature κ, or torsion τ, of the helix in the case where κ and τ are much smaller than the inverse of the interatomic distance. More specifically, we have found that the EMF components acting on the binormal and tangential components of $\hat{\boldsymbol{L}}_{\tilde{k}}$ are proportional to κ and τ, respectively.

We have confirmed such geometry dependence by calculating the current-induced polarizations of $\hat{\boldsymbol{L}}_n$ and the spin at each atom. We have shown, in the region of small κ and τ, that binormal and tangential components of current-induced polarizations are proportional to κ and τ, respectively.

ACKNOWLEDGMENTS

This work was supported by Grant-in-Aid for Scientific Research (C) Grant No. JP21K03413 from the Japan Society for the Promotion of Science (JSPS).

AUTHOR DECLARATIONS

Conflict of Interest

The authors have no conflicts to disclose.

Author Contributions

Yuya Yatabe: Conceptualization (equal); Data curation (lead); Formal analysis (equal); Investigation (equal); Methodology (equal); Validation (equal); Visualization (lead); Writing – original draft (supporting); Writing – review & editing (supporting). **Hiroshi Akera**: Conceptualization (equal); Formal analysis (equal); Funding acquisition (lead); Investigation (equal); Methodology (equal); Supervision (lead); Validation (equal); Visualization (supporting); Writing – original draft (lead); Writing – review & editing (lead).

DATA AVAILABILITY

The data that support the findings of this study are available within the article.

REFERENCES

[1] S. G. Ray, S. S. Daube, G. Leitus, Z. Vager, and R. Naaman, "Chirality-induced spin-selective properties of self-assembled monolayers of DNA on gold," Phys. Rev. Lett. **96**, 036101 (2006).
[2] B. Göhler, V. Hamelbeck, T. Z. Markus, M. Kettner, G. F. Hanne, Z. Vager, R. Naaman, and H. Zacharias, "Spin selectivity in electron transmission through self-assembled monolayers of double-stranded DNA," Science **331**, 894–897 (2011).
[3] Z. Xie, T. Z. Markus, S. R. Cohen, Z. Vager, R. Gutierrez, and R. Naaman, "Spin specific electron conduction through DNA oligomers," Nano Lett. **11**, 4652–4655 (2011).
[4] D. Mishra, T. Z. Markus, R. Naaman, M. Kettner, B. Göhler, H. Zacharias, N. Friedman, M. Sheves, and C. Fontanesi, "Spin-dependent electron transmission through bacteriorhodopsin embedded in purple membrane," Proc. Natl. Acad. Sci. U. S. A. **110**, 14872–14876 (2013).
[5] M. Kettner, B. Göhler, H. Zacharias, D. Mishra, V. Kiran, R. Naaman, C. Fontanesi, D. H. Waldeck, S. Sek, J. Pawłowski, and J. Juhaniewicz, "Spin filtering in electron transport through chiral oligopeptides," J. Phys. Chem. C **119**, 14542–14547 (2015).
[6] V. Kiran, S. P. Mathew, S. R. Cohen, I. Hernández Delgado, J. Lacour, and R. Naaman, "Helicenes—A new class of organic spin filter," Adv. Mater. **28**, 1957–1962 (2016).
[7] A. C. Aragonès, E. Medina, M. Ferrer-Huerta, N. Gimeno, M. Teixidó, J. L. Palma, N. Tao, J. M. Ugalde, E. Giralt, I. Díez-Pérez, and V. Mujica, "Measuring the spin-polarization power of a single chiral molecule," Small **13**, 1602519 (2017).
[8] M. Kettner, V. V. Maslyuk, D. Nürenberg, J. Seibel, R. Gutierrez, G. Cuniberti, K.-H. Ernst, and H. Zacharias, "Chirality-dependent electron spin filtering by molecular monolayers of helicenes," J. Phys. Chem. Lett. **9**, 2025–2030 (2018).
[9] H. Lu, J. Wang, C. Xiao, X. Pan, X. Chen, R. Brunecky, J. J. Berry, K. Zhu, M. C. Beard, and Z. V. Vardeny, "Spin-dependent charge transport through 2D chiral hybrid lead-iodide perovskites," Sci. Adv. **5**, eaay0571 (2019).
[10] S. Mishra, A. K. Mondal, S. Pal, T. K. Das, E. Z. B. Smolinsky, G. Siligardi, and R. Naaman, "Length-dependent electron spin polarization in oligopeptides and DNA," J. Phys. Chem. C **124**, 10776–10782 (2020).
[11] T. Liu, X. Wang, H. Wang, G. Shi, F. Gao, H. Feng, H. Deng, L. Hu, E. Lochner, P. Schlottmann, S. von Molnár, Y. Li, J. Zhao, and P. Xiong, "Linear and nonlinear two-terminal spin-valve effect from chirality-induced spin selectivity," ACS Nano **14**, 15983–15991 (2020).
[12] R. Naaman and D. H. Waldeck, "Spintronics and chirality: Spin selectivity in electron transport through chiral molecules," Annu. Rev. Phys. Chem. **66**, 263–281 (2015).
[13] C. Kulkarni, A. K. Mondal, T. K. Das, G. Grinbom, F. Tassinari, M. F. J. Mabesoone, E. W. Meijer, and R. Naaman, "Highly efficient and tunable filtering of electrons' spin by supramolecular chirality of nanofiber-based materials," Adv. Mater. **32**, 1904965 (2020).
[14] R. Otsuto, Y. Yatabe, and H. Akera, "Orbital and spin polarizations induced by current through a helical atomic chain," Phys. Rev. B **104**, 035431 (2021).
[15] S. Varela, V. Mujica, and E. Medina, "Effective spin-orbit couplings in an analytical tight-binding model of DNA: Spin filtering and chiral spin transport," Phys. Rev. B **93**, 155436 (2016).
[16] Y. Utsumi, O. Entin-Wohlman, and A. Aharony, "Spin selectivity through time-reversal symmetric helical junctions," Phys. Rev. B **102**, 035445 (2020).
[17] J. C. Slater and G. F. Koster, "Simplified LCAO method for the periodic potential problem," Phys. Rev. **94**, 1498–1524 (1954).
[18] T. Ando, "Spin-orbit interaction in carbon nanotubes," J. Phys. Soc. Jpn. **69**, 1757–1763 (2000).
[19] P. Carrier and S.-H. Wei, "Calculated spin-orbit splitting of all diamondlike and zinc-blende semiconductors: Effects of $p_{1/2}$ local orbitals and chemical trends," Phys. Rev. B **70**, 035212 (2004).

[20]D. Rybkovskiy, A. Osadchy, and E. Obraztsova, "Electronic band structure of helical iodine chains," Phys. Status Solidi B **249**, 2608–2611 (2012).
[21]W. Izumida, K. Sato, and R. Saito, "Spin-orbit interaction in single wall carbon nanotubes: Symmetry adapted tight-binding calculation and effective model analysis," J. Phys. Soc. Jpn. **78**, 074707 (2009).
[22]S. R. Park, C. H. Kim, J. Yu, J. H. Han, and C. Kim, "Orbital-angular-momentum based origin of Rashba-type surface band splitting," Phys. Rev. Lett. **107**, 156803 (2011).
[23]S. Oh and H. J. Choi, "Orbital angular momentum analysis for giant spin splitting in solids and nanostructures," Sci. Rep. **7**, 2024(2017).
[24]J. H. Ryoo and C.-H. Park, "Hidden orbital polarization in diamond, silicon, germanium, gallium arsenide and layered materials," NPG Asia Mater. **9**, e382 (2017).
[25]D. Go, J.-P. Hanke, P. M. Buhl, F. Freimuth, G. Bihlmayer, H.-W. Lee, Y. Mokrousov, and S. Blügel, "Toward surface orbitronics: Giant orbital magnetism from the orbital Rashba effect at the surface of sp-metals," Sci. Rep. **7**, 46742 (2017).